IOPscience iopscience.iop.org

Home Search Collections Journals About Contact us My IOPscience

A study of the spatial structure of turbulent flow by intensity-fluctuation spectroscopy

This article has been downloaded from IOPscience. Please scroll down to see the full text article.

1970 J. Phys. A: Gen. Phys. 3 216

(http://iopscience.iop.org/0022-3689/3/2/013)

View the table of contents for this issue, or go to the journal homepage for more

Download details:
IP Address: 171.66.16.71
The article was downloaded on 02/06/2010 at 04:14

Please note that terms and conditions apply.

A study of the spatial structure of turbulent flow by intensity-fluctuation spectroscopy

P. J. BOURKE†, J. BUTTERWORTH†, L. E. DRAIN†,
P. A. EGELSTAFF†, A. J. HUGHES‡, P. HUTCHINSON†,
D. A. JACKSON§, E. JAKEMAN‡, B. MOSS†,
J. O'SHAUGHNESSY‡, E. R. PIKE‡ and P. SCHOFIELD†

† Atomic Energy Research Establishment, Harwell, Didcot, Berks.
‡ Royal Radar Establishment, Malvern, Worcs.
§ University of Kent at Canterbury, Kent

MS. received 24th September 1969

Abstract. The spectrum of intensity fluctuations of laser light scattered from small particles in a turbulent water flow has been used to investigate the spatial distribution of velocity. Data on the spatial correlation and ergodicity of turbulence, not previously available by hot wire anemometry, have been obtained.

1. Introduction

The measurement of the velocity distribution at a point in turbulent flow of water through a tube (by laser light-beating spectroscopy) has been reported by Goldstein and Hagen (1967) and by Pike *et al.* (1968). In these experiments the Doppler-shift technique was used: light scattered from particles in the water was mixed with a reference beam from the laser at the cathode of a photomultiplier. Since the scattered light is Doppler-shifted by an amount proportional to the component of the particle velocity parallel to the scattering vector (the difference in wave vector of the incident and scattered light), the observed spectrum gives a direct measure of the distribution of velocities in the fluid. The spectra were found to be approximately Gaussian and the root-mean-square deviations from the mean velocities, obtained as a function of the Reynolds number, were in close agreement with those found from conventional hot-wire anemometry. Further experiments of this kind are reported here; in these the Reynolds number was fixed and the size of the region under study was varied.

In addition, we report the observation of the spatial correlation of velocities at different points within the water, by applying intensity-fluctuation spectroscopy (Siegert 1943, Forrester *et al.* 1955, Alkemade 1959, Alpert *et al.* 1965, Ford and Benedek 1965) to the light scattered from particles in the water. The observed spectrum arises from the distribution of the differences of Doppler shifts from pairs of particles and hence its average frequency is zero. In addition, there is a line of negligible width at zero frequency arising from the intensity of light scattered from single particles. The volume of water in which light capable of beating with the reference beam is scattered is limited by criteria of optical coherence to ensure good mixing at the photocathode. In these experiments this volume could be varied from 'the order of' to small compared with the correlation range for the turbulent velocity distribution in the fluid. As this volume is reduced to be smaller than the correlation range the spectrum should narrow owing to the positive correlations of velocities at short distances. A brief account of this work has been published (Bourke *et al.* 1969).

Since the publication of our earlier paper (Pike *et al.* 1968) a theoretical account of the optical spectrum of scattering from turbulent flow has appeared (Bertolotti *et al.* 1969). In the present paper we extend the theory to derive the spectrum of intensity fluctuations of the scattered light and we also include for completeness the Doppler case, which gives the optical spectrum directly. The theory may be regarded as a

generalization to directions other than back-scattering of the work of Siegert (1943) in radar intensity-fluctuation spectroscopy of atmospheric turbulence. Light scattered by the particles is detected by a photomultiplier whose output is fed into a spectrum analyser. The signal strength in a chosen frequency band is then measured. Particles entering the illuminated volume are detected after a delay given by the reciprocal bandwidth of the spectrum analyser, and continue to be monitored while they remain in the volume and continue to move with a velocity which maintains the Doppler shift of the scattered light within limits determined by the bandwidth.

The theoretical analysis is based on the following set of assumptions:

(i) The main contribution to the observed spectrum is from light scattered by particles suspended in the fluid (either naturally occurring or specially introduced in the form of polystrene balls). This is confirmed visually. Scattering from the pure fluid depends on the change in refractive index with density and on the compressibility. This scattering is very small compared with the scattering from particles which depends on the difference in refractive index between particles and fluid.

(ii) The particles move with a velocity equal to the local velocity of the surrounding fluid. That is, the rate of motion of particles through the fluid is small compared with the rate of transport by the turbulent velocity. This is also well satisfied in this experiment.

(iii) Each particle scatters a negligible part of the incident beam, and the distance between particles is large compared with the wavelength. This means that the scattering of light from a number of particles can be calculated as the sum of scatterings from single particles, and that multiple scattering can be neglected. This requires that the density of particles should be sufficiently low.

(iv) There is no spatial correlation between particles, and the number contributing to the time-averaged light intensity at a given frequency is very large. This implies that the velocity distribution in the fluid is sampled uniformly so that we can relate the time-averaged scattering from the particles to the ensemble average of the turbulent velocity distribution.

(v) The uncertainty introduced by the finite time a particle spends in the visible region of the fluid (the so-called ambiguity broadening) can be neglected (see § 4).

(vi) It is assumed that a particle maintains its velocity within limits set by the wave analyser bandwidth for a time long compared with the reciprocal of the corresponding frequency.

Assumption (vi) is the main limitation on the straightforward interpretation of the experiments. It is discussed in § 5. The predictions of the theory are given in § 3.

The experimental method and the corrections applied to the data are described in §§ 4 and 5 respectively. Experimental measurements of Doppler spectra and of intensity-fluctuation spectra are presented in § 6 and discussed in § 7.

2. Theory

We consider the scattering produced by a particle suspended in a fluid which has a trajectory $\boldsymbol{r}(t)$ relative to some origin inside an illuminated region, seen by the detector, of volume V. The magnitude of the electric field in the scattered wave at a position $\boldsymbol{R}$ at a large distance from the particle may be written

$$E_s(\boldsymbol{R}, t) = \frac{E_I(\boldsymbol{r}, t)\alpha \exp(ik|\boldsymbol{R}-\boldsymbol{r}|)}{|\boldsymbol{R}-\boldsymbol{r}|} \tag{1}$$

where $\boldsymbol{E}_I(r, t)$ is the electric field vector of the incident light beam and $\boldsymbol{k}$ the wave vector of the scattered light (which is parallel to $\boldsymbol{R}$). α represents a complex scattering amplitude associated with the particle. For a particle of a size of the order of, or larger than, the wavelength of the light, α depends on a number of factors, such as the

scattering angle, orientation of the particle and polarization of the light. In this paper we are not concerned with the details of the scattering process, however, and α will be regarded as an arbitrary parameter.

The incident field is written

$$E_{\mathrm{I}} = E_0 \exp\{-\mathrm{i}(\omega t - \boldsymbol{k}_0 \cdot \boldsymbol{r})\}. \tag{2}$$

We define a function $\theta(t)$

$$\begin{aligned} \theta(t) &= 1 \qquad \text{if } \boldsymbol{r}(t) \text{ is inside } V \\ &= 0 \qquad \text{otherwise.} \end{aligned} \tag{3}$$

Then the scattered field from a single particle is, from (1) and (2),

$$E_{\mathrm{s}}(\boldsymbol{R}, t) = \frac{E_0 \alpha \exp(\mathrm{i}kR)}{|\boldsymbol{R} - \boldsymbol{r}|} \theta(t) \exp[-\mathrm{i}\{\omega t + \boldsymbol{\kappa} \cdot \boldsymbol{r}(t)\}] \tag{4}$$

where $\boldsymbol{\kappa}$ is the scattering vector $\boldsymbol{k} - \boldsymbol{k}_0$ and $k|\boldsymbol{R} - \boldsymbol{r}(t)|$ has been approximated by $kR - \boldsymbol{k} \cdot \boldsymbol{r}(t)$ for $\boldsymbol{R}$ at a large distance from the visible region.

The detected signal is obtained by integrating the field over the collection surface at the photocathode of the detector. This surface is taken to be the coherence area of two scattered beams at the photocathode (see § 4). We may thus define a 'detected' amplitude from a single particle

$$\hat{E} = a \exp(\mathrm{i}\phi) = \int_{\mathrm{s}} \mathrm{d}A \frac{E_0 \alpha \exp(\mathrm{i}kR)}{|\boldsymbol{R} - \boldsymbol{r}|} \tag{5}$$

where a is the real amplitude of the integral of the field over the detection surface and ϕ an associated phase.

Next we write correspondingly for a reference beam (having the same wavelength as the incident beam)

$$E(t) = \hat{E}_0 \exp(-\mathrm{i}\omega_0 t) = a_0 \exp\{-\mathrm{i}(\omega_0 t - \phi_0)\}. \tag{6}$$

Thus, labelling the particles by subscript p and making assumption (iii) which allows us to sum the fields calculated for single particles, we obtain for the positive frequency part of the total field at the photocathode

$$E(t) = a_0 \exp\{-\mathrm{i}(\omega_0 t - \phi_0)\} + \sum_p a_p \theta_p(t) \exp[-\mathrm{i}\{\omega_0 t + \boldsymbol{\kappa} \cdot \boldsymbol{r}_p(t)\} + \mathrm{i}\phi]. \tag{7}$$

The probability of annihilation of a photon at the photocathode is proportional to the squared modulus of $E(t)$ (Glauber 1963). Consequently the output of the photomultiplier is proportional to

$$\begin{aligned} |E(t)|^2 = {} & {a_0}^2 + \sum_p {a_p}^2 \theta_p(t) + 2a_0 \sum_p a_p \theta_p(t) \cos\{\phi_0 - \phi_p + \boldsymbol{\kappa} \cdot \boldsymbol{r}_p(t)\} \\ & + \sum_{p \neq p'} a_p a_{p'} \theta_p(t) \theta_{p'}(t) \exp[-\mathrm{i}\boldsymbol{\kappa} \cdot \{\boldsymbol{r}_p(t) - \boldsymbol{r}_{p'}(t)\} + \mathrm{i}(\phi_p + \phi_{p'})]. \end{aligned} \tag{8}$$

In the experimental arrangement described in § 4, a particular frequency Ω is selected with a wave analyser of response time T_{A}. The observed spectrum $S(\Omega)$ is then the time average of the square modulus of the angular output

$$S(\Omega) = \left\langle \frac{1}{T_{\mathrm{A}}} \left| \int_{\tau}^{\tau + T_{\mathrm{A}}} |E(t)|^2 \exp(\mathrm{i}\Omega t)\, \mathrm{d}t \right|^2 \right\rangle \tag{9}$$

the angular brackets denoting an average over the observation times τ. In the following we make assumptions (v) and (vi):

(*a*) We assume that a particle remains in the visible region throughout the interval $(\tau, \tau+T_A)$. Then under the integral in (9) we can write $\theta(t) = \theta'(\tau)$, where $\theta'(\tau)$ is unity if the particle is in the visible region during the interval and zero otherwise.

(*b*) We assume $T_A \gg \Omega^{-1}$. This allows us to replace the lower limits of integration by $-\infty$ and take the limit $T_A \to \infty$.

(*c*) We assume that the velocity of a particle does not change appreciably during a time T_A. Thus we replace $\boldsymbol{\kappa} \cdot \{\boldsymbol{r}_p(t) - \boldsymbol{r}_{p'}(t')\}$ by $(t-t')\kappa v_p{}^\kappa$ for $|t-t'| \leqslant T_A$, where $v_p{}^\kappa$ is the component of the velocity of the particle in the direction of the scattering vector $\boldsymbol{\kappa}$ (assumption (vi)). Then we obtain

$$\begin{aligned}\frac{1}{T_A}\left|\int_\tau^{\tau+T_A} |E(t)|^2 \exp(i\Omega t)\,dt\right|^2 \simeq\ & 2\pi\{a_0{}^2 + \sum_p \theta_p'(\tau) a_p{}^2\}^2 \delta(\Omega) \\ & + 2\pi a_0{}^2 \sum_p \theta_p'(\tau) a_p{}^2 \{\delta(\Omega + \kappa v_p{}^\kappa) + \delta(\Omega - \kappa v_p{}^\kappa)\} \\ & + 2\pi \sum_p \sum_{p \neq p'} \theta_p'(\tau)\theta_{p'}'(\tau) a_p{}^2 a_{p'}{}^2 \\ & \times \delta\{\Omega - \kappa(v_p{}^\kappa - v_{p'}{}^\kappa)\} \\ & + \text{ terms involving } \exp[i\{\phi_p + \boldsymbol{\kappa} \cdot \boldsymbol{r}_p(t)\}]. \end{aligned} \quad (10)$$

In order to observe the spectrum, we require the bandwidth to be small compared with $\kappa\bar{v}$, where $\bar{v}$ is the r.m.s. turbulent velocity, but we also require that its inverse is small compared with the period the particle velocity remains unchanged. The validity of these assumptions in the experiments reported here is discussed in § 5.4, where it is shown that the second is only marginally satisfied.

The final stage is to perform the average over successive values of τ. We now invoke assumptions (ii) and (iv). Since the velocity of a particle is determined by the fluid flow, it is uncorrelated with a_p. If bars denote averages over the particles, we have

$$\begin{aligned} S(\Omega) = {} & 2\pi[a_0{}^4 + 2a_0{}^2\overline{a_p{}^2}\langle N(\tau)\rangle + \overline{(a_p{}^2)^2}\langle\{N(\tau)\}^2\rangle + \{\overline{a_p{}^4} - \overline{(a_p{}^2)^2}\}\langle N(\tau)\rangle]\,\delta(\Omega) \\ & + \frac{2\pi}{\kappa} a_0{}^2 \overline{a_p{}^2}\langle n_u(\tau) + n_{-u}(\tau)\rangle \\ & + \frac{2\pi}{\kappa}\overline{(a_p{}^2)^2}\left[\int_{-\infty}^{\infty} dv\ \langle n_v(\tau) n_{v+u}(\tau)\rangle - \langle N(\tau)\rangle\delta(u)\right] \end{aligned} \quad (11)$$

where

$$\begin{aligned} u &= \frac{\Omega}{\kappa} \\ n_u(\tau) &= \sum_p \theta_p'\delta(v_p{}^\kappa - u) \end{aligned} \quad (12)$$

$N(\tau)$ is the number of particles present in the visible region at any time:

$$N(\tau) = \sum_p \theta_p(\tau) = \int_{-\infty}^{\infty} dv\, n_v(\tau). \quad (13)$$

If the turbulence is statistically stationary and assumption (iv) is valid, so that the visible region is sampled uniformly by the particles, then the time average over the velocities may be replaced by ensemble averages over the probability distribution of velocities in the fluid. Let $P_0(v^\kappa, \boldsymbol{r})$ be the probability of velocity v^κ at $\boldsymbol{r}$ and

$P_1(v_1^\kappa, v_2^\kappa; \boldsymbol{r}_1, \boldsymbol{r}_2)$ the joint distribution of simultaneously having velocity v_1^κ at $\boldsymbol{r}_1$ and v_2^κ at $\boldsymbol{r}_2$. Then

$$\langle n_u \rangle = \langle N \rangle \frac{1}{V} \int_V \mathrm{d}^3\boldsymbol{r} \int_{-\infty}^{\infty} \mathrm{d}v^\kappa P_0(v^\kappa, \boldsymbol{r}) \delta(v^\kappa - u) \tag{14}$$

and

$$\begin{aligned} \langle n_v n_{v+u} \rangle = {} & \langle N^2 \rangle \frac{1}{V^2} \int_V \mathrm{d}^3\boldsymbol{r}_1 \int_V \mathrm{d}^3\boldsymbol{r}_2 \int_{-\infty}^{\infty} \mathrm{d}v_1^\kappa \int_{-\infty}^{\infty} \mathrm{d}v_2^\kappa \\ & \times P_1(v_1^\kappa, v_2^\kappa; \boldsymbol{r}_1, \boldsymbol{r}_2) \delta(v_1^\kappa - v) \delta(v_2^\kappa - v - u) \\ & + \langle N \rangle \frac{1}{V} \int_V \mathrm{d}^3 r_1 \int_{-\infty}^{\infty} \mathrm{d}v_1^\kappa P_0(v_1^\kappa, \boldsymbol{r}_1) \delta(u). \end{aligned} \tag{15}$$

We may here assume translational invariance of the velocity correlations as the scattering volume has only a small radial extent compared with the variation of the mean flow, and is located far from the tube entrance (§ 4). Equations (14) and (15) then simplify to

$$\langle n_u(\tau) \rangle = \langle N \rangle P_0(u) \tag{16}$$

$$\langle n_v(\tau) n_{u+v}(\tau) \rangle = \langle N^2 \rangle \frac{1}{V} \int_V d\boldsymbol{r}\, P_1(v, u+v; \boldsymbol{r}) + \langle N \rangle \delta(u). \tag{17}$$

3. Theoretical predictions

The spectrum given by equation (11) may be separated into a Doppler spectrum (D.s.) and an intensity-fluctuation spectrum (i.f.s.). In the Doppler spectrum we assume $a_0^2 \gg \langle N \rangle \overline{a_p^2}$ and all terms not containing a_0^2 may be neglected. The intensity fluctuation spectrum is observed in the absence of the reference beam, so that for this case we set a_0^2 equal to zero. Thus

$$S_{\mathrm{Ds}}(\Omega) = 2\pi a_0^2 (a_0^2 + 2\langle N \rangle a_p^2) \delta(\Omega) + \frac{2\pi}{\kappa} a_0^2 \overline{a_p^2} \langle N \rangle \{P_0(u) + P_0(-u)\} \tag{18}$$

and

$$\begin{aligned} S_{\mathrm{ifs}}(\Omega) = {} & 2\pi [(\overline{a_p^2})^2 \langle N^2 \rangle + \{a_p^4 - (\overline{a_p^2})^2\} \langle N \rangle] \delta(\Omega) \\ & + \frac{2\pi}{\kappa} (\overline{a_p^2})^2 \langle N^2 \rangle \frac{1}{V} \int_V \mathrm{d}^3 r \int_{-\infty}^{\infty} \mathrm{d}v\, P_1(v, v+u; \boldsymbol{r}). \end{aligned} \tag{19}$$

If we consider a single side band of the Doppler spectrum we note that use of equation (14) gives

$$\langle \Omega^2 \rangle_{\mathrm{Ds}} - \langle \Omega \rangle_{\mathrm{Ds}}^2 = \kappa^2 \{ \langle (v^\kappa)^2 \rangle - \langle v^\kappa \rangle^2 \}. \tag{20}$$

Similarly, neglecting the central delta function in the i.f.s. case gives

$$\langle \Omega^2 \rangle_{\mathrm{ifs}} - \langle \Omega \rangle_{\mathrm{ifs}}^2 = 2\kappa^2 \left\{ \langle (v^\kappa)^2 \rangle - \frac{1}{V} \int_V \mathrm{d}^3 \boldsymbol{r} \langle v_1^\kappa \, . \, v_2^\kappa \rangle \right\}. \tag{21}$$

When the scattering volume is large compared with the correlation range for velocities $\langle v_1^\kappa v_2^\kappa \rangle$ will be independent of separation over the bulk of the scattering volume and equation (21) reduces to

$$\lim_{V_{\mathrm{sc}} \to \infty} (\langle \Omega^2 \rangle_{\mathrm{ifs}} - \langle \Omega \rangle_{\mathrm{ifs}}^2) = 2\kappa^2 \{ \langle (v^\kappa)^2 \rangle - \langle v^\kappa \rangle^2 \} = 2(\langle \Omega^2 \rangle_{\mathrm{Ds}} - \langle \Omega \rangle^2). \tag{22}$$

It should be noted that the variance of the i.f.s. approaches twice that of the D.s., *independently* of the spectral shape, for large scattering volume. A consequence of this is that (20) and (21) are correct even if assumption (vi) is invalid.

The probability distribution $P_0(v^x)$, in a fully developed turbulent flow is well approximated by a Gaussian (Batchelor 1958) and it is immediately clear that the Doppler spectrum should be well fitted by a Gaussian. However, the wings of the i.f.s. are also well fitted by a Gaussian for a scattering volume whose axial extent is of the order of the correlation range (§ 6), and the width of this Gaussian approaches $\sqrt{2}$ times the D.s. width. If we consider two volume elements separated by the correlation range and situated on the extrema of the visible volume we obtain a contribution to the i.f.s. given by

$$\Delta S(\Omega)_{\mathrm{ifs}} = \frac{4\pi^2}{\kappa}\overline{(a_p{}^2)^2}\frac{\langle N\rangle^2}{V^2}(\Delta V)^2\int_{-\infty}^{+\infty} dv\, P_0(v)P_0(v+u). \tag{23}$$

As is well known, the convolution of two Gaussians is a Gaussian with a width broadened by a factor $\sqrt{2}$. As the wings of the i.f.s. are determined by the maximum velocity differences existing in the scattering volume we may expect contributions from the extrema of V_{sc} to dominate. Consequently equation (23) predicts a Gaussian shape to the wings of the i.f.s. and a relatively rapid approach of the width of this Gaussian to $\sqrt{2}$ times the D.s. width. This factor is well known in the radar work mentioned above (see, for example, Atlas 1964). However, the complete equation (19) is required to discuss the i.f.s. as a function of scattering volume.

4. Experimental apparatus

The apparatus is shown diagramatically in figure 1. A beam from a helium–neon laser ($\lambda = 6328$ Å) was passed through a beam splitter to give a signal beam and a reference beam. The signal beam passed through a lens (focal length 20 cm) to focus at a point A. The reference beam was reflected from a mirror, as shown in figure 1,

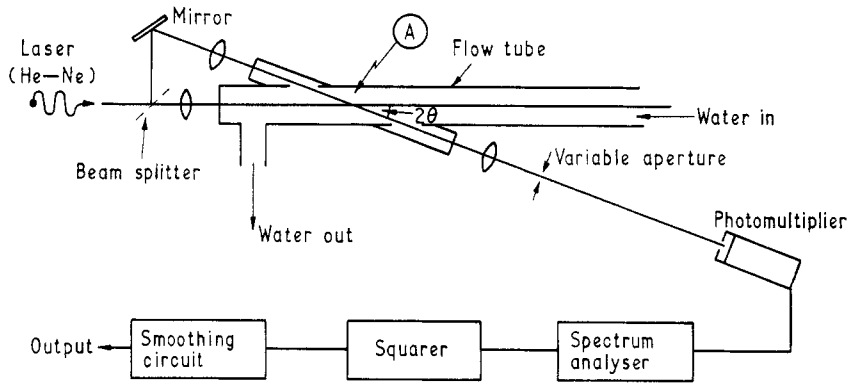

Figure 1. Diagrammatic sketch of the apparatus. The point A marks the intersection of the signal and reference beams and defines the sample of turbulent liquid being studied.

and passed through a second lens (also 20 cm focal length) to focus at A. The angle 2θ between the two beams was 16° (or 11°) at the point of intersection. A glass tube (13 mm diameter and 1·03 m length or 4 mm diameter and 50 cm length), closed with a glass plate at one end, was placed with its axis along the signal beam, so that the point A was situated at 70 tube diameters from the open end. The larger tube was fitted with glass side arms (2 mm diameter) through which the reference beam passed and these were closed with glass end plates. The smaller tube was passed through a wide copper tube filled with water, through which the reference beam passed. Water was passed into the tube, at the open end, and out through a side arm located at the

blanked-off end approximately 13 cm from the point A. This arrangement was chosen so that at the position of measurement (i.e. the intersection of the reference and signal beams some 70 tube diameters from the inlet and 10 diameters from the outlet) fully developed fluid velocity profiles had been established. There was therefore no change in mean velocity through the volume in which the velocity measurements were being made.

A third lens of 10 cm focal length was placed in the line of the reference beam to produce a full-sized image of the signal beam at twice its focal length away from itself. This was done so that variable apertures could be placed on this image to control accurately the length of signal beam visible to the photomultiplier (this length is given by the diameter of the aperture divided by $\sin 2\theta$). A photomultiplier (type EMI 9558), with a 0·35 mm diameter pinhole on its cathode, was positioned 150 cm away from the image.

To obtain a good mixing, the scattered and reference light should produce not more than (approximately) half an interference fringe across the cathode, i.e.

$$\alpha \leqslant \frac{\lambda}{2d} \tag{24}$$

where α is the angle between wave fronts of scattered and reference light, λ is the wavelength and d the photocathode diameter. This requirement defines a cone of coherence with its apex on the cathode and of semi-apex angle α. The only light capable of beating strongly with the reference beam is that scattered within this cone. It is therefore the intercept of the signal beam (in the water) by this cone, which defines the volume in which the velocity is being measured. The diameter of the cone of coherence at the image of the signal beam was 2 mm, which was larger than the biggest pinhole placed on the image. Therefore, for all measurements, the length of the signal beam over which the turbulent velocities were being measured was controlled by the pinhole diameter and was not further restricted by the cone of coherence.

In one arrangement the detection apparatus was similar to that described previously (Pike *et al.* 1968). The multiplier output was fed, via a wide band amplifier, to a Tektronix 1L5 wave analyser. The instrument was set to scan the frequency range (0 to 50 kHz or 0 to 150 kHz) of interest in a time of two minutes. The resolution of the spectrum analyser could be pre-set in the range 10 to 500 Hz. The output from its rectification stage was fed through a Burr-Brown squaring circuit into an RC averaging circuit with a one-second time constant. The spectra were displayed on an oscilloscope for initial adjustments and then recorded on an XY plotter for quantitative measurements.

In another arrangement the detecting system was set up as shown in figure 2(*a*). The output from the wave analyser was squared, passed to an analogue to digital converter and then to a multi-channel scaler. For a typical run 50 channels were used, with 200 ms per channel per sweep (equivalent to 3 kHz/channel) and 30 sweeps were added together. Figure 2(*b*) shows a typical result from this equipment.

The apparatus was aligned using the reference beam. With this beam, Doppler-spectrum measurements were made. For i.f.s. measurements the only change needed was to block off the reference beam. Measurements were made with ordinary tap water and also with demineralized water flowing through the tube. In the tap water the naturally occurring solid contamination scattered sufficient light. Polyvinyl-chloride balls of $0{\cdot}7 \pm 0{\cdot}1$ μm diameter were added in the demineralized water to a concentration such that more than 90% of the beat signal was produced from light scattered by those balls. The flow was controlled by a constant-head tank. For the experiments using the 13 mm tube, a flow of 45 $cm^3\ s^{-1}$ at 20 °C with a mean axial centre line velocity of 36 $cm\ s^{-1}$ was used and the aperture on the image of the signal beam was varied using a series of pinholes of diameters between 0·1 and 2·0 mm.

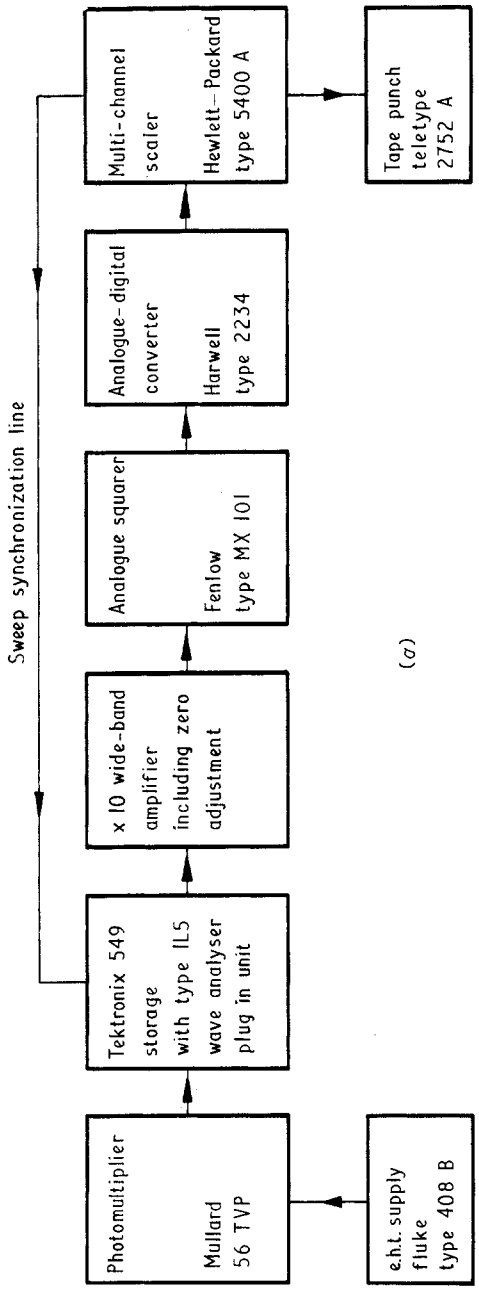

Figure 2(*a*). Block diagram of the detecting system used for digital analysis of data. A multi-channel scaler is used for signal integration.

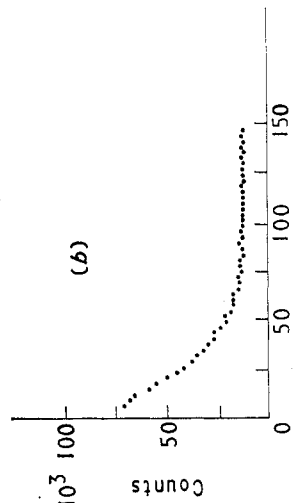

Figure 2(*b*). Intensity-fluctuation spectrum observed with the apparatus of figure 2(*a*) using a scattering angle of 11° and summing 30 scans, each of 10 s duration.

5. Sources of error

5.1. *Doppler ambiguity broadening*

The finite 'lifetime' of Doppler-shifted signals from individual scattering particles in the water due to their short times of passage through the signal beam produces a broadening of the spectra analogous to the Doppler radar ambiguity. With the present arrangement the lifetimes of signals from individual particles may be limited either to the length of beam visible to the multiplier divided by the mean axial velocity, or to the average width of the beam divided by the r.m.s. radial velocity. With the smallest (0·1 mm) pinhole, the former lifetime was 10^{-3} s. With a 20 cm focal length lens giving a beam waist diameter of 50 μm (Pike *et al.* 1968) and taking the r.m.s. radial velocity to be 4% of the mean axial velocity (Laufer 1952), the average value of the latter lifetime was also about 10^{-3} s. For i.f.s. measurements when the signal is dependent on two particles staying in the beam, its lifetime may be taken as $0{\cdot}5 \times 10^{-3}$ s, i.e. half the above value.

In the previous work (Pike *et al.* 1968) it was shown that the relationship between this lifetime (τ) and the r.m.s. spectral width ($\Delta\nu$) was

$$\Delta\nu \simeq \frac{1}{2\tau} \tag{25}$$

or about 1 kHz in the present case.

All the observed spectra were Gaussian (see § 6) with r.m.s. widths of 5·0 kHz or greater. Hence, taking the observed mean squares to be the sum of the mean squares due to both velocity fluctuations and ambiguous broadening, the error in the observed r.m.s. widths due to the ambiguity effect was less than 2%. The above reasoning was checked as previously (Pike *et al.* 1968) by tests with laminar flow to obtain the ambiguity spectra directly. These spectra were as predicted and since their effect was small it has been neglected in analysis of the results. This is contained in the function θ_p in equation (4) and was neglected in equation (8). Analogous arguments may be used to justify the neglect of particle rotation broadening of the spectra.

5.2. *Variation in scattering angle*

A further correction arises (Goldstein and Hagen 1967) due to the broadening effect on the spectra of the variation in scattering angle of light arriving at the multiplier. The wave front of the signal beam at its waist is planar (Born and Wolf 1959) so that there can be no variation in the direction of incident light across the beam. The direction of scattered light can, however, vary (see figure 1) by the angle subtended at the cathode by the pinhole on the image of the signal beam. With the biggest (2·0 mm) pinhole used this angle was 0·06°. The nominal scattering angle was 16°; hence the r.m.s. broadening of the spectra due to this effect may be taken as approximately 0·003 times the D.s. peak frequency, i.e. about 0·09 kHz. Again this is negligible compared with the observed r.m.s. spectral widths of 5·0 kHz or greater. This reasoning was also confirmed by the laminar flow tests mentioned above.

5.3. *Subtraction of noise*

A part of the observed spectra is a background arising from stray light and from fluctuations in the phototube and the detecting system. In the case of the squared spectra the subtraction of the noise n from the required signal s is straightforward since

$$\langle |n+s|^2 \rangle = \langle |n|^2 \rangle + \langle |s|^2 \rangle. \tag{26}$$

The cross term vanishes since n and s are oscillatory quantities uncorrelated in phase.

5.4. *Non-rectilinear motion of particles*

It turns out that the main limitation in interpreting the results in accordance with the analysis of § 2 relates to the time a particle moves with unchanging velocity. The

period of the turbulent fluctuation can be estimated from the diameter of the tube and the fluid velocity, in terms of the Fourier components of the velocity spectrum. Examination of Laufer's data (Laufer 1952) suggests the condition (ii) in § 1 is satisfied by the larger wavelength components but not by the whole spectrum. This means that the finer scale of the turbulence is not observed by this technique. However, this is a limitation which also applied to hot-wire techniques involving a tracking filter with the same response time (T_A).

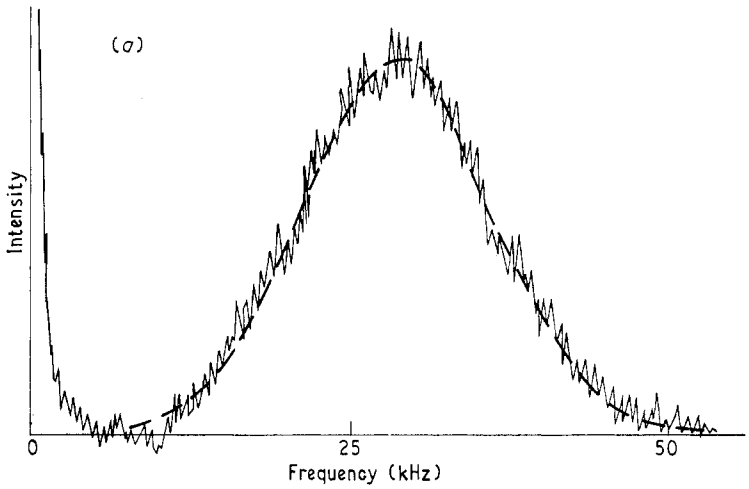

Figure 3(*a*). Typical spectrum for the Doppler case taken on the XY plotter. The noise has been subtracted from the data and the peak at zero frequency arises from the beating of the reference beam with itself. The broken curve is a Gaussian fit to the spectrum. $\sigma = 7{\cdot}8$ kHz.

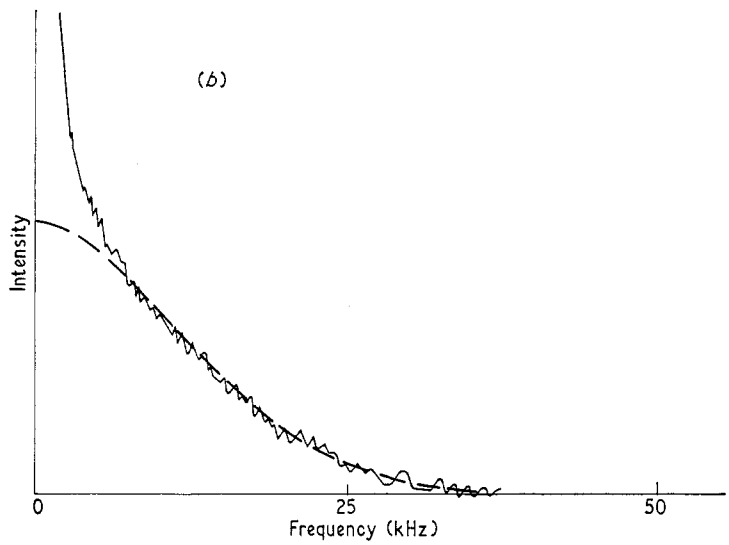

Figure 3(*b*). Typical spectrum of the intensity fluctuations taken on the XY plotter. The peak at zero frequency arises from the self-beating of light scattered by a single particle, while the wings of the spectrum arise from light scattered by pairs of particles. Noise has been subtracted and the broken curve is a Gaussian distribution fitted to the wings of the curve. $\sigma = 11{\cdot}4$ kHz.

6. Results

Typical spectra are shown in figure 3(*a*)–Doppler case, and in figure 3(*b*)–intensity-fluctuation case, for water loaded with polyvinylchloride balls and a resolution of 500 Hz. In the i.f.s. case there is a large narrow central peak superimposed on a broad spectrum, corresponding respectively to the first and third terms in equation (11). The broken lines on these figures represent the best Gaussian fit to the curves. These curves are fitted in the D.s. case to the whole spectrum and in the i.f.s. case to the wings of the broader spectrum where the influence of the narrow central peak has become insignificant. It can be seen that the observed spectra are Gaussian (in the wings) within experimental error.

From equation (2) the frequency shift is related to velocity by the equation

$$\left.\begin{aligned} \Delta\omega &= 2\pi\Omega = \boldsymbol{\kappa} \cdot \boldsymbol{v} \\ \text{or} \qquad v^{\kappa} &= \frac{\lambda_1 \Omega}{2 \sin\theta} \\ \text{and} \qquad v_{\text{axial}} &= \frac{v^{\kappa}}{\sin\theta} \end{aligned}\right\} \tag{27}$$

where λ_1 is the wavelength of the light in the water (i.e. λ/n) and θ is half the scattering angle† (here Ω is in Hz rather than rad s^{-1} in equation (9)). The mean axial velocity calculated from the peak frequency of the D.s. spectra and equation (27) agreed to within 3% with the value calculated from the measured flow rate and known velocity profiles (Roftus *et al.* 1957).

The standard deviation of $P_0(V^{\kappa})$—equation (20)—is known from hot-wire anemometry (Bourke *et al.* 1968) and so allows the r.m.s. width of the squared Doppler spectrum to be given as 9 ± 1 kHz for the larger tube. Table 1 summarizes the present measurements of this quantity.

Table 1. r.m.s. width of Doppler spectrum for 13 mm tube

Visible length of beam (cm)	Spectrum analyser resolution (Hz)	Squared width (kHz)
0·19	500	9·0 ± 0·3
0·19	50	8·8 ± 0·4
0·95	500	8·5 ± 0·3
0·95	10	8·4 ± 0·4

All these data were taken using demineralized water loaded with polyvinylchloride balls. For Doppler-shift measurements individual balls are being monitored and so the ergodic theorem may be used to equate volume and time averages‡. A resolution of 10 Hz corresponds to a time average over 0·055 s, or 2 cm of fluid passing at the mean flow rate. Thus the cases in table 1 cover lengths of 0·15 to 2 tube diameters, and confirm the constancy of the squared width. The mean value is 8·6 ± 0·2 kHz.

The i.f.s case was studied for visible lengths from 0·1 to 0·95 cm at a resolution of 500 Hz, which corresponds to a time average over 1 ms. In this experiment the

† This angle is unchanged by the transition from water to air because of the construction of the side arms (figure 1).

‡ This hypothesis cannot be applied to the i.f.s. case where pairs of particles must be considered.

distribution of instantaneous velocity differences between pairs of particles is examined and the distribution (as a function of time) is integrated over the response time of the analyser. The relaxation time for velocity change in the flow (t_T) is about 20 ms, i.e. t_T is much greater than the analyser response time (T_A). These data (analysed as in figure 3) are presented in figure 4. It can be seen that the data from the two types of

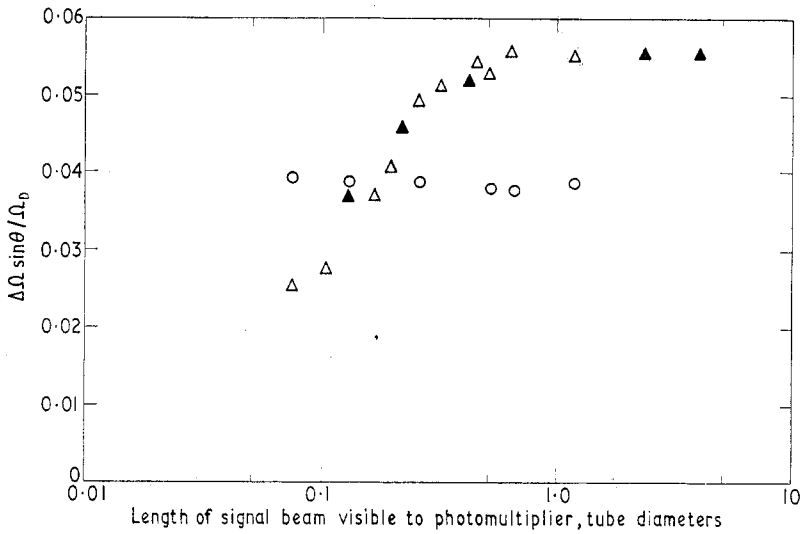

Figure 4. Variation of spectral width with visible length for Doppler and intensity fluctuation spectra. $\Delta\Omega$ is the standard deviation of S_p and Ω_D is the peak frequency observed in the Doppler experiment. Doppler spectrum: ○ tube diameter 13 mm, Re No. 4000, $\theta = 8°$. Intensity-fluctuation spectrum: △ tube diameter 13 mm, Re No. 4000, $\theta = 8°$; ▲ tube diameter 3·5 mm, Re No. 3800, $\theta = 5{\cdot}5°$.

scattering particle are in good agreement and also that the data from the two tube sizes agree. At a length of about one tube diameter the data are consistent with the limit given in equation (22). At visible lengths less than 0·7 of a tube diameter the width falls off owing to the spatial correlation of velocities over this size range. The shape of this curve is directly related to the spatial correlation function in the axial direction of the component of turbulent velocity in an almost radial direction as discussed in § 2. It shows that the correlation has fallen to near zero at (about) half a tube diameter. There appear to be no data in the literature for comparison.

7. Discussion and conclusions

In this paper, we have outlined the theory of the spectrum of light scattered from particles carried by a turbulent fluid, and reported preliminary experiments which indicate that this is a viable technique for the study of both turbulent velocity distributions, and spatial correlations of turbulent velocities.

The velocity distribution has been measured by what we have called the Doppler-shift technique where the scattered light is mixed with a reference beam; the low-frequency spectrum gives a fairly direct measure of the distribution of Doppler shifts from the scattering particles. The results here are in excellent agreement with those obtained by hot-wire anemometry. This agreement incidentally confirms the equivalence of space and time averages in turbulence along the axis of a tube—as is to be expected from the ergodic hypothesis.

The second type of experiment, entitled 'intensity fluctuation spectroscopy', mixes light scattered from pairs of particles at different points within the fluid; the spectrum gives the distribution of differences in the Doppler shifts from pairs of particles. In the present experiments these are within the same illuminated region.

We have studied how the width of the intensity-fluctuation spectrum varies with the size of the visible region, varying this from 0·1 to 5·0 times the tube diameter. This width increases by a factor of about 2 as the visible length increases from 0·1 to 0·5 tube diameters, after which it remains constant at a value which is $\sqrt{2}$ times the Doppler width as predicted by the theory. This approach to the asymptotic value at about half the tube diameter is in accord with the range of the turbulence being smaller than the tube diameter, or in other words that the largest turbulence eddies are smaller than the tube diameters.

The variation in spectral width with illuminated volume contains information about the axial correlation of radial velocities. Further work is in progress to analyse the data to obtain more quantitative information about this correlation. Such correlation has not been previously measured with the hot-wire technique because of the difficulty in working with two X probes.

References

ALKEMADE, C. T. J., 1959, *Physica*, **25,** 1145–58.
ALPERT, S. S., YEH, Y., and LIPWORTH, E., 1965, *Phys. Rev. Lett.*, **14,** 486–8.
ATLAS, D., 1964, *Adv. Geophys.*, **10,** 317–488.
BATCHELOR, G. K., 1958, *Homogeneous Turbulence* (London: Cambridge University Press).
BERTOLOTTI, M., GROSIGNANI, B., DI PORTO, P., and SETTE, D., 1969, *J. Phys.* A: *Gen. Phys.*, **2,** 126–8.
BORN, M., and WOLF, E., 1959, *Principles of Optics* (New York: Pergamon Press).
BOURKE, P. J., *et al.*, 1969, *Phys. Lett.*, **28A,** 692–3.
BOURKE, P. J., PULLING, D. J., GILL, L. E., and DENTON, W. M., 1968, *Proc. Instn Mech. Engrs*, **182,** 58–68
FORD, N. C., and BENEDEK, G. B., 1965, *Phys. Rev. Lett.*, **15,** 649–51.
FORRESTER, A. T., GUDMUNSEN, R. A., and JOHNSON, P. O., 1955, *Phys. Rev.*, **99,** 1691–700.
GLAUBER, R. J., 1963, *Phys. Rev.*, **130,** 2529–39.
GOLDSTEIN, R. J., and HAGEN, W. F., 1967, *Phys. Fluids*, **10,** 1349–50.
LAUFER, J., 1952, *N.A.C.A. Rep.* No. TN 1175.
PIKE, E. R., JACKSON, D. A., BOURKE, P. J., and PAGE, D. I., 1968, *J. Phys.* E: *Sci. Instrum.*, **1,** 727–30.
ROFTUS, A., ARCHER, D. H., KLIMAS, I. C., and SIKCHI, K. G., 1957, *A.I.Ch.E.J.*, **3,** 208–16.
SIEGERT, A. J. F., 1943, *M.I.T. Rad. Lab. Rep.*, No. 465.

J. PHYS. A: GEN. PHYS., 1970, VOL. 3. PRINTED IN GREAT BRITAIN